Normal-Mode Characteristics of Chlorophyll Models. Vibrational Analysis of Metallooctaethylchlorins and Their Selectively Deuterated Analogues

Harold N. Fonda,[†] W. Anthony Oertling,[‡] Asaad Salehi,[§] Chi K. Chang,* and Gerald T. Babcock*

Contribution from the Department of Chemistry and the LASER Laboratory, Michigan State University, East Lansing, Michigan 48824-1322. *Received January 29, 1990*

Abstract: The resonance Raman (RR) and infrared (IR) spectra of the Zn, Cu, and Ni complexes of *trans*-octaethylchlorin (OEC) reveal significant differences in the vibrational-mode properties of metallochlorins and metalloporphyrins. Modes with a contribution from the C_aC_m stretching coordinate are distinguished by their sensitivity to metal substitution and to selective d_2 and d_4 methine deuteration. Comparison of the resonance Raman spectrum of CuOEC with that of CuECI (ECI = etiochlorin I) identifies those modes with a contribution from C_bC_b and C_bC_s stretching and C_bC_s bending coordinates. The results obtained show that there is substantial mixing of C_aC_m and C_bC_b stretching character in the high-frequency modes of MOEC. The suggestion[21] that the symmetry reduction that occurs in metallochlorins relative to metalloporphyrins produces vibrational-mode localization to specific hemispheres or quadrants of the macrocycle has been tested and confirmed by specific d_2 deuteration at the methine carbons. Resonance Raman spectra of CuOEP-d_2 (OEP = octaethylporphyrin) and CuOEP-d_4 establish that, for a delocalized mode, methine d_2 deuteration can be expected to produce half the d_4 shift. For CuOEC, selective deuteration at the α,β and γ,δ methine positions causes different patterns of frequency shifts that indicate the extent of mode localization. Analysis of these data shows that the normal modes of the MOEC class of compounds have varying degrees of localization; moreover, it identifies those modes that retain delocalized, porphyrin-like behavior, albeit with altered potential energy distributions relative to the MOEP situation. In agreement with the analysis by Boldt et al., however, we find that, in general, it is not possible to assign the vibrational modes of metallochlorins by direct analogy with metalloporphyrins. An exception to this occurs for several modes below 1350 cm^{-1} that are localized in the α,β positions away from the reduced pyrole ring, but modes that are γ,δ localized in this frequency region have no porphyrin counterparts.

Introduction

Resonance Raman spectroscopic studies of metalloporphyrins and hemoproteins[1] have benefited from the availability of a consistent set of vibrational-mode assignments based on the normal-coordinate analysis of NiOEP (nickel(II) octaethylporphyrin).[2] In contrast, metallochlorins have received less attention, and a consensus on their characteristic vibrational properties has yet to emerge (for a recent review, see ref 3). Metallochlorins occur in a variety of biological systems including the chlorophyll pigments of higher plants,[4] leukocyte myeloperoxidase,[5] and bacterial heme *d*-containing enzymes.[6] With the crystallization of the photosynthetic bacterial reaction center[7] and the possibility of carrying out static and time-resolved vibrational spectroscopy on the events involved in primary-charge separation, there is a strong motivation for developing a consistent vibrational analysis of metallochlorin and metallobacteriochlorin macrocyles. Establishment of unambiguous vibrational-mode assignments for highly symmetric metallooctaethylchlorins (MOEC) (Figure 1) is a necessary first step in this process and is essential to the analysis of the more complex natural systems.[4,5,8-10]

Reduction of a C_bC_b bond in a metalloporphyrin to form a metallochlorin lowers the molecular symmetry from D_{4h} to C_2 and has a profound effect on the structure of the entire macrocycle.[3] Comparative X-ray crystalographic study[11] of Fe^{II}OEP and Fe^{II}OEC shows that, while the two complexes have similar core sizes (1.996 vs 1.986 Å), the porphyrin macrocycle is planar but the chlorin macrocycle is S_4 ruffled. A variety of Raman studies has been carried out on metallochlorins, and the results have provided considerable insight into the effects that symmetry reduction has on the vibrational properties of the macrocycle.[12-20] Andersson et al., for example, have assigned the phenyl modes of ZnTPP, ZnTPC, and ZnTPiBC on the basis of symmetry arguments.[12] An important issue that has become apparent in this work is whether chlorin normal modes can be assigned in

[†] Present address: Department of Chemistry, Colorado State University, Fort Collins, CO 80523.

[‡] Present address: Chemistry Department, University of California, Santa Barbara, CA 93106.

[§] Present address: INC/4, Mail Stop C-345, Los Alamos National Laboratory, Los Alamos, NM 87545.

(1) (a) Felton, R. H.; Yu, N.-T. In *The Porphyrin*; Dolphin, D., Ed.; Academic Press: New York, 1979; Vol. III, pp 347-393. (b) Spiro, T. G. In *Iron Porphyrins*; Lever, A. B. P., Gray, H. B., Eds.; Addison-Wesley: Reading, MA, 1983; Part 2, pp 89-159. (c) Kitagawa, T.; Ozaki, Y. *Struct. Bonding (Berlin)* **1987**, *64*, 71-114. (d) Babcock, G. T. In *Biological Applications of Raman Spectroscopy*; Spiro, T. G., Ed.; Wiley: New York, 1988; Vol. 3, pp 293-346.

(2) (a) Abe, M.; Kitagawa, T.; Kyogoku, Y. *J. Chem. Phys.* **1978**, *69*, 4526-4534. (b) Kitagawa, T.; Abe, M.; Ogoshi, H. *J. Chem. Phys.* **1978**, *69*, 4516-4525. (c) Abe, M. In *Spectroscopy of Biological Systems*; Clark, R. J. H., Hester, R. E., Eds.; Wiley: London, 1986; pp 347-393. (d) Gladkov, L. L.; Solovyov, K. N. *Spectrochim. Acta, Part A* **1986**, *42A*, 1-10. (e) Li, X.-Y.; Czernuszewicz, R. S.; Kincaid, J. R.; Stein, P.; Spiro, T. G. *J. Phys. Chem.* **1990**, *94*, 47-61.

(3) Schick, G. A.; Bocian, D. F. *Biochim. Biophys. Acta* **1987**, *895*, 127-154.

(4) Svec, W. A. In *The Porphyrins*; Dolphin, D., Ed.; Academic Press: New York, 1979; Vol. V, pp 341-399.

(5) (a) Sibbet, S. S.; Hurst, J. K. *Biochemistry* **1984**, *23*, 3007-3013. (b) Babcock, G. T.; Ingle, R. T.; Oertling, W. A.; Davis, J. C.; Averill, B. A.; Hulse, C. L.; Stufkens, D. J.; Bolscher, B. G. J. M.; Wever, R. *Biochim. Biophys. Acta* **1985**, *828*, 58-66.

(6) (a) Timkovich, R.; Cork, M. S.; Gennis, R. B.; Johnson, P. Y. *J. Am. Chem. Soc.* **1985**, *107*, 6069-6075. (b) Chang, C. K. *J. Biol. Chem.* **1985**, *260*, 9520-9522. (c) Chang, C. K.; Wu, W. *J. Biol. Chem.* **1986**, *261*, 8593-8596.

(7) (a) Deisenhofer, J.; Epp, O.; Miki, K.; Huber, R.; Michel, H. *J. Mol. Biol.* **1984**, *180*, 385-398. (b) Chang, C.-H.; Schiffer, M.; Tiede, D.; Smith, U.; Norris, J. *J. Mol. Biol.* **1985**, *186*, 201-203. (c) Allen, J. P.; Feher, G.; Yeates, T. O.; Komiya, H.; Rees, D. C. *Proc. Natl. Acad. Sci. U.S.A.* **1987**, *84*, 6162-6166. (d) Michel, H.; Deisenhoffer, J. *Biochemistry* **1988**, *27*, 1-7. (e) Deisenhofer, J.; Michel, H. *Science* **1989**, *245*, 1463-1473.

(8) (a) Lutz, M. *C. R. Acad. Sci. Paris* **1972**, *B275*, 497-500. (b) Lutz, M.; Breton, J. *Biochim. Biophys. Res. Commun.* **1973**, *53*, 413-418. (c) Lutz, M. *J. Raman Spectrosc.* **1974**, *2*, 497-516. (d) Lutz, M. In *Lasers in Physical Chemistry and Biophysics*; Joussof-Dubien, J., Ed.; Elsevier: Amsterdam, 1975; pp 451-463. (e) Lutz, M. *Biochim. Biophys. Acta* **1977**, *460*, 408-430. (f) Lutz, M.; Brown, J. S.; Remy, R. In *Chlorophyll Organization and Energy Transfer in Photosynthesis*; Wolstenholme, G., Fitzsimons, D. W., Eds.; Excerpta Medica: Amsterdam, 1979; pp 105-125. (g) Lutz, M. In *Advances in Infrared and Raman Spectroscopy*; Clark, R. J. H., Hester, R. E., Eds.; Wiley Heyden: London, 1983; Vol. 11, pp 211-300. (h) Lutz, M.; Robert, B. In *Biological Applications of Raman Spectroscopy*; Spiro, T. G.; Ed.; Wiley: New York, 1988; Vol. 3, pp 347-411.

0002-7863/90/1512-9497$02.50/0

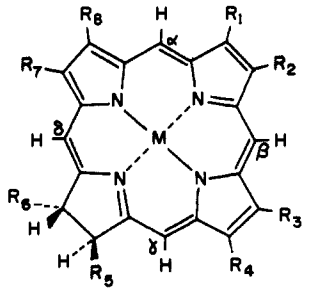

MOEC: R_1–R_8 = C_2H_5 M = Zn, Cu, Ni

MECI: R_1, R_3, R_5, R_7 = CH_3 M = Cu

R_2, R_4, R_6, R_8 = C_2H_5

Figure 1. Structural formula and labeling scheme for *trans*-metallooctaethylchlorin (MOEC) and *trans*-metalloetiochlorin (MECI).

analogy with those that occur in metalloporphyrins. Boldt et al.[21] have argued that such an approach is not appropriate. In their resonance Raman study of NiOEC, which was supported by normal-coordinate calculations, they concluded that the metallochlorin normal modes were substantially altered. A key conclusion from this work was that a number of modes in the reduced ring macrocycle appear to be localized rather than delocalized over the whole macrocycle as occurs in the case of metalloporphyrins.

A detailed test of the normal-mode assignments of metallochlorins has been difficult, owing to the complexity of the system and to the differing objectives of the studies performed to date. Ozaki et al.[13] reported solution resonance Raman spectra for CuOEC, CuOEC-γ,δ-d_2, CuOEC-$^{15}N_4$, NiOEC, Fe^{III}OECX (X = F^-, Cl^-), and $Fe^{III}OECIm_2$ with Q_x excitation at 488.0 nm. Their observations were later extended to include a variety of FeOEC complexes in various spin, oxidation, and ligation states.[14] Although this work revealed that the vibrations of metallochlorins were somewhat different from those of metalloporphyrins, it did not firmly establish normal-mode assignments. Andersson et al. have studied a number of metallochlorin model compounds, including Fe^{III}pPP,[16] Fe^{III}DC,[16] NiTMC,[17] CuTPC,[17] Cu–diol chlorin,[18] Cu–lactone chlorin,[18] and Cu–$(Me)_7$chlorin.[18] The goal of this work was the identification of the influences arising from chlorin macrocyclic substituents, particularly those with physiological significance, but the necessary variation in peripheral substituents in these complexes obscures the assignment of the fundamental vibrational modes of the chlorin macrocycle itself. Boldt et al.[21] performed a normal-coordinate analysis for NiOEC and obtained resonance Raman spectra of NiOEC and some of its specifically deuterated isotopomers with Soret, Q_x, and Q_y excitation. Support for their assignments also came from comparison with the resonance Raman spectra of Cu–diol chlorin-d_4 in KBr recorded by Andersson et al.[18] Further analysis of these normal-coordinate calculations was limited, however, by the unavailability of key isotopically labeled forms of OEC. More recently, the Bocian group has reported resonance Raman data for monomeric and oxygen-bridged dimeric FeOEC[22] as well as for Cu^{II}TPC and copper(II) tetraphenylbacteriochlorin.[23]

Table I. Electronic Absorption Maxima (nm) for MOEC Complexes in Benzene Solution

	absorption maxima (nm)						
complex	Soret	Q_{x01}	Q_{x00}	Q_{y02}	Q_{y01}	Q_{y00}	r^a
ZnOEC	401	502	538	572	590	617	0.08
CuOEC	400	495	530	571	591	614	0.09
NiOEC	398	491	523	571	590	615	0.13

[a] r is the ratio of the Q_{y00} to Soret band oscillator strengths.

In this work, we present the IR and resonance Raman spectra of solution samples of ZnOEC, CuOEC, NiOEC, CuECI (Figure 1), and several selectively methine-deuterated CuOEC complexes obtained with Soret, Q_x, and Q_y excitation. Both IR and resonance Raman spectra are necessary to characterize fully the metallochlorin vibrational modes. By using the symmetric M^{II}OEC complexes, we avoid the reliance on a single metal and the complications introduced by other peripheral substitutents. Metal substitution with Zn, Cu, and Ni covers a wide range of core sizes without introducing the ligand, spin, and oxidation state effects associated with the Fe complexes. The amounts of C_aC_m and C_bC_b stretching character in the core size sensitive modes are distinguished by the sensitivity of the vibrational frequency to metal substitution. Comparison of the spectra of CuOEC and CuECI identifies those modes with a contribution from C_bC_b and C_bC_s (s = substituent) stretching and C_bC_s bending coordinates as in the case with the analogous porphyrin species.[24] The frequency shifts observed for CuOEC upon d_4, as well as α,β-d_2 and γ,δ-d_2 methine deuteration, confirm our mode assignments and permit assessment of the extent of localization for a given mode. The use of CuOEC, CuOEC-α,β-d_2, CuOEC-γ,δ-d_2, and CuOEC-d_4 allows more accurate assignment of many of the normal modes than was previously possible. The results we obtain support the concept of mode localization introduced by Boldt et al.,[21] although the mode composition for some modes differs somewhat from that deduced in their analysis.

Experimental Section

Preparation of Complexes. *trans*-H_2OEC and *trans*-H_2ECI were prepared from Fe^{III}(OEP)Cl and Fe^{III}(EPI)Cl, respectively, by reduction with sodium metal in isoamyl alcohol.[25] Chromatography on alumina (Grade I) with benzene–ether (9:1, v/v) was used to eliminate any residual free-base porphyrin.[26] The copper and zinc complexes were prepared by standard metal-insertion methods[27] and purified by chromatography on silica gel with benzene. NiOEC was obtained as described[21] with the addition of chromatography on silica gel as a final step.

H_2OEC-d_4 was prepared by treatment of H_2OEC with D_2SO_4–D_2O (9:1, v/v).[28] Reduction of the D_2SO_4 to D_2O ratio to 6:1 afforded H_2OEC-γ,δ-d_2.[29] Reexchange at the γ,δ methine positions of H_2OEC-d_4

(9) Cotton, T. M.; Timkovich, R.; Cork, M. S. *FEBS Lett.* **1981**, *133*, 39–44.
(10) Ching, Y.; Ondrias, M. R.; Rousseau, D. L.; Mohoberic, B. B.; Wharton, D. C. *FEBS Lett.* **1982**, *138*, 239–244.
(11) Strauss, S. H.; Silver, M. E.; Long, K. M.; Thompson, R. G.; Hudgens, R. A.; Spartalian, K.; Ibers, J. A. *J. Am. Chem. Soc.* **1985**, *107*, 4207–4215.
(12) Andersson, L. A.; Loehr, T. M.; Thompson, R. G.; Strauss, S. H. *Inorg. Chem.* **1990**, *29*, 2142–2147.
(13) Ozaki, Y.; Kitagawa, T.; Ogoshi, H. *Inorg. Chem.* **1978**, *18*, 1772–1776.
(14) (a) Ozaki, Y.; Iriyama, K.; Ogoshi, H.; Ochiai, T.; Kitagawa, T. *J. Phys. Chem.* **1986**, *90*, 6105–6112. (b) Ozaki, Y.; Iriyama, K.; Ogoshi, H.; Ochiai, T.; Kitagawa, T. *J. Phys. Chem.* **1986**, *90*, 6113–6118.
(15) Andersson, L. A.; Loehr, T. M.; Chang, C. K.; Mauk, A. G. *J. Am. Chem. Soc.* **1985**, *107*, 182–191.
(16) Andersson, L. A.; Loehr, T. M.; Lim, A. R.; Mauk, A. G. *J. Biol. Chem.* **1984**, *259*, 15340–15349.
(17) Andersson, L. A.; Loehr, T. M.; Sotiriou, C.; Wu, W.; Chang, C. K. *J. Am. Chem. Soc.* **1986**, *108*, 2908–2916.
(18) Andersson, L. A.; Sotiriou, C.; Chang, C. K.; Loehr, T. M. *J. Am. Chem. Soc.* **1987**, *109*, 258–264.
(19) Loehr, T. M.; Andersson, L. A.; Sotiriou, C.; Wu, W.; Chang, C. K.; Simpson, D. J.; Smith, K. M.; Stershic, M.; Stolzenberg, A. M. *Rec. Trav. Chim. Pays-Bas* **1987**, *106*, 328.
(20) Andersson, L. A.; Loehr, T. M.; Cotton, T. M.; Simpson, D. J.; Smith, K. M. *Biochim. Biophys. Acta* **1989**, *974*, 163–179.
(21) Boldt, N. J.; Donohoe, R. J.; Birge, R. R.; Bocian, D. F. *J. Am. Chem. Soc.* **1987**, *109*, 2284–2298.
(22) Boldt, N. J.; Bocian, D. F. *J. Phys. Chem.* **1988**, *92*, 581–586.
(23) Donohoe, R. J.; Atamian, M.; Bocian, D. F. *J. Phys. Chem.* **1989**, *93*, 2244–2252.
(24) Oertling, W. A.; Salehi, A.; Chang, C. K.; Babcock, G. T. *J. Phys. Chem.* **1989**, *93*, 1311–13.
(25) Whitlock, H. W., Jr.; Hanover, R.; Oester, M. Y.; Bower, B. K. *J. Am. Chem. Soc.* **1969**, *91*, 7485–7489.
(26) Eisner, V.; Linstead, R. P.; Parkes, E. A.; Stephen, E. *J. Chem. Soc.* **1956**, 1655–1661.
(27) Falk, J. E. *Porphyrins and Metalloporphyrins*; Elsevier: New York, 1964; p 798.
(28) Bonnett, R.; Stephenson, G. F. *Proc. Chem. Soc.* **1964**, 291.
(29) Salehi, A.; Fonda, H. N.; Oertling, A. W.; Babcock, G. T.; Chang, C. K. *J. Labelled Compd. Radiopharm.* **1988**, *25*, 1333–1337.

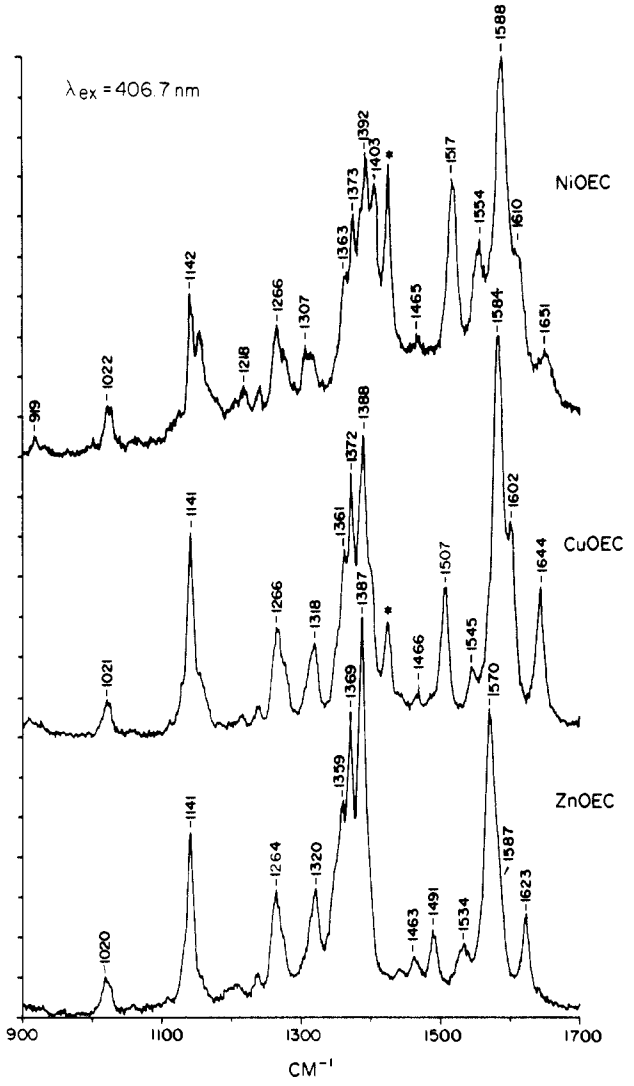

Figure 2. Resonance Raman spectra of ZnOEC, CuOEC, and NiOEC in CH_2Cl_2 solution obtained with Soret excitation at 406.7 nm. Laser powers: 5, 7, and 20 mW, respectively. Concentrations: 200, 36, and 76 μM, respectively.

with H_2SO_4–H_2O (6:1, v/v) produced H_2OEC-α,β-d_2.[26] The proton NMR spectrum of *trans*-H_2OEC shows two peaks at 9.7 and 8.9 ppm corresponding to the α,β and γ,δ hydrogens, respectively. Deuteration at the α,β positions is seen by disappearance of the 9.7 ppm peak and at the γ,δ positions by disappearance of the 8.9 ppm peak. In H_2OEC-d_4 both signals are absent. Deuterium substitution is quantitative for H_2OEC-d_4 and H_2OEC-γ,δ-d_2. H_2OEC-α,β-d_2 showed 90% deuteration at the α,β positions and complete proton recovery at the γ,δ positions.[29]

CuOEP and CuOEP-d_4 were prepared from H_2OEP and H_2OEP-d_4,[28] respectively. CuOEP-d_2 was prepared from CuOEC-γ,δ-d_2 by treatment with a solution of 2,3-dichloro-5,6-dicyanoquinone in benzene.[30] The complexes were purified by chromatography on silica gel with CH_2Cl_2.

Spectral Measurements. Electronic absorption spectra were recorded for solutions of the metallochlorins in benzene on a Perkin-Elmer Lambda 5 UV-vis spectrometer. Infrared spectra were recorded for CCl_4 solutions in a 0.2-mm-pathlength cell with NaCl windows at 2-cm^{-1} resolution on a Perkin-Elmer Model 1750 FTIR spectrometer. Raman spectra were obtained on a computer-controlled Spex 1401 double monochromator equipped with photon-counting electronics. Excitation at 406.7 nm was provided by a Coherent Model 90K krypton ion laser, at 488.0 nm by a Spectra Physics Model 165 argon ion laser, and at 615.0 nm by Rhodamine 590 laser dye in an argon ion pumped Spectra Physics Model 375 dye laser. Data were collected at 1-cm^{-1} intervals with a 1-s dwell time and with 5-cm^{-1} resolution. Measured depolarization ratios are accurate to ±0.1. The Raman spectrum of ZnOEC in CH_2Cl_2 was obtained on a degassed sample sealed in a quartz EPR tube under argon. Spectra of CuOEC and NiOEC were obtained for CH_2Cl_2 solutions contained in a cylindrical quartz spinning cell and in KBr disks. Actual laser powers employed are noted in the figure captions.

(30) Eisner, U. *J. Chem. Soc.* **1957**, 3461–3469.

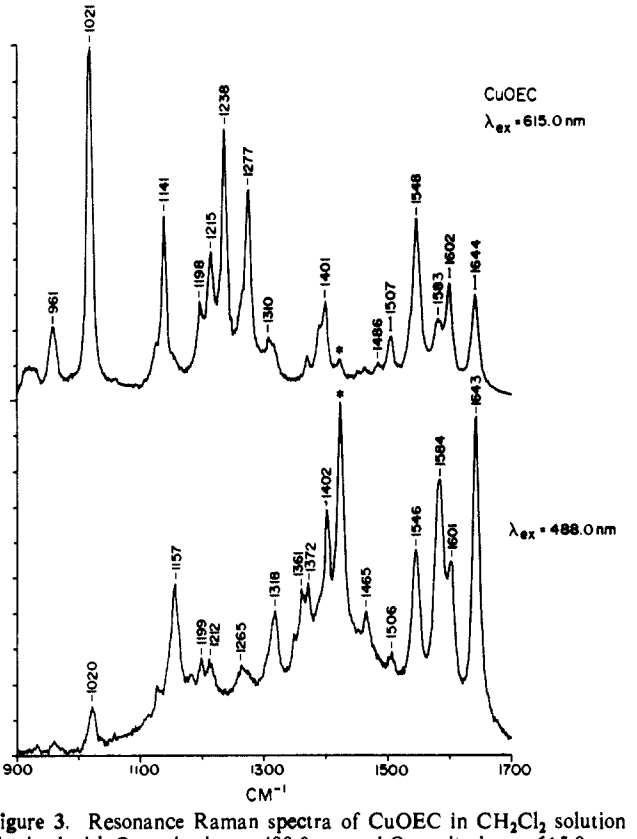

Figure 3. Resonance Raman spectra of CuOEC in CH_2Cl_2 solution obtained with Q_x excitation at 488.0 nm and Q_y excitation at 615.0 nm. Laser powers: 100 and 35 mW, respectively. Concentrations: 790 and 68 μM, respectively.

Results

Electronic Absorption Spectra. The electronic absorption spectra of ZnOEC, CuOEC, and NiOEC in benzene solution display the characteristic features of metallochlorins, namely, separate Q_x and Q_y transitions (and vibronic sidebands) with the peak absorbance of the Q_{y00} band about half that of the Soret absorption band. The absorption maxima are listed in Table I together with the ratio of the Q_{y00} to Soret oscillator strengths, r, for each complex. The oscillator strength ratios were determined by measuring the areas under the Soret and Q_{y00} bands for the absorption spectra plotted on a wavenumber scale. The energies of the Soret and Q_x transitions follow the order Ni > Cu > Zn. In the Gouterman four-orbital model[31] for alkyl-substituted metalloporphyrins the porphyrin a_{2u} orbital is lower in energy than the a_{1u} orbital. The a_{2u} orbital has the appropriate symmetry to interact with the metal π orbitals. As the metal becomes more electropositive, the ionic radius increases causing expansion of the macrocycle core and the energy of the a_{2u} orbital is raised relative to the a_{1u} orbital. This results in a red-shift of the Soret and Q bands and a decrease in the ratio of the Q to Soret oscillator strengths. The absorptions of the MOEC complexes behave in the same manner, although the oscillator strength ratios are larger than the respective MOEP complexes, reflecting the allowed nature of the Q_y transition in metallochlorins.

Resonance Raman Spectra of MOEC. The resonance Raman spectra of ZnOEC, CuOEC, and NiOEC in CH_2Cl_2 solution obtained with Soret excitation at 406.7 nm are shown in Figure 2. The vibrational frequencies for these species and the depolarization ratios for CuOEC are listed in Table II. Five modes in the frequency region from 1490 to 1700 cm^{-1}, corresponding to the 1644-, 1602-, 1584-, 1545-, and 1507-cm^{-1} modes of CuOEC, are observed to be metal dependent. Inspection of the

(31) (a) Gouterman, M. *J. Chem. Phys.* **1958**, *30*, 1139–1161. (b) Gouterman, M. *J. Molec. Spectrosc.* **1961**, *6*, 138–163.

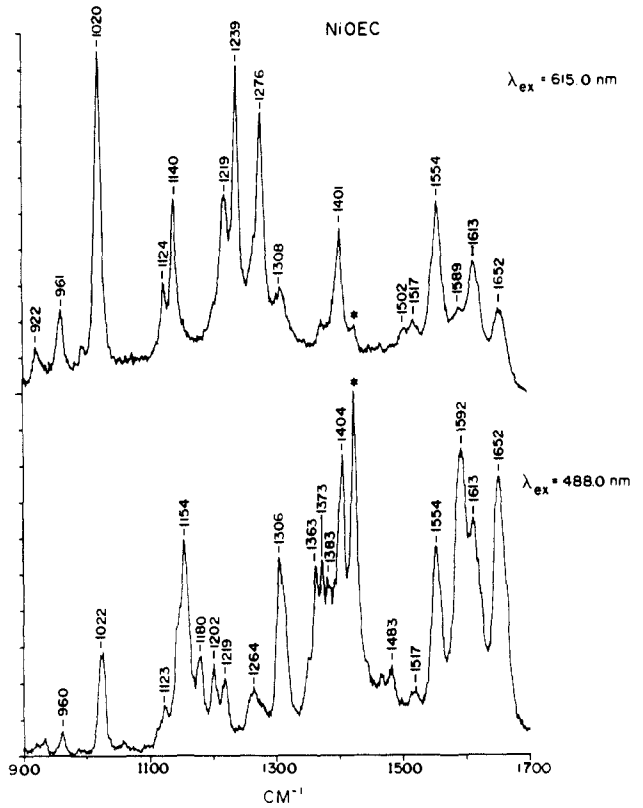

Figure 4. Resonance Raman spectra of NiOEC in CH_2Cl_2 solution obtained with Q_x excitation at 488.0 nm and Q_y excitation at 615.0 nm. Laser powers: 70 and 40 mW, respectively. Concentrations: 1.1 mM and 96 μM, respectively.

polarized resonance Raman spectra of CuOEC at 406.7 nm (now shown) reveals that the 1545-cm^{-1} band consists of a 1547-cm^{-1} polarized mode and a 1543-cm^{-1} anomalously polarized mode.

Resonance Raman spectra of CuOEC (Figure 3) and NiOEC (Figure 4) in CH_2Cl_2 solution were obtained with Q_x excitation at 488.0 nm and with Q_y excitation at 615.0 nm. The intense fluorescence of ZnOEC prohibited the measurement of its resonance Raman spectra with visible excitation. The frequencies are listed in Table II along with the depolarization ratios for CuOEC. The 488.0-nm excitation spectra agree with those reported by Ozaki et al.[13] For CuOEC, bands that are not seen with Soret excitation are observed at 1199, 960, and 932 cm^{-1} with Q_x and Q_y excitation; at 1182 cm^{-1} with Q_x excitation only; and at 1486, 1310, and 923 cm^{-1} with Q_y excitation only. The 1486-cm^{-1} band of CuOEC is metal sensitive, corresponding to the 1502-cm^{-1} mode of NiOEC observed with Q_y excitation.

IR Spectra of MOEC. For a metallochlorin of C_2 symmetry, the resonance Raman active modes are also IR active. The IR spectra of ZnOEC, CuOEC, and NiOEC in CCl_4 solution are shown in Figure 5, and the vibrational frequencies are listed in Table II. The total number of bands observed by IR spectroscopy is greater than with resonance Raman spectroscopy as a result of IR activity of the internal vibrations of the ethyl groups. These modes can be identified by comparison of the spectra in Figure 5 to the IR spectrum of NiOEP reported by Kincaid et al.[32] The two closely spaced modes at 1543 and 1547 cm^{-1} of CuOEC that can be resolved in the Raman spectrum by depolarization ratio measurement are apparent in the IR spectrum; similarly, the 1534-cm^{-1} resonance Raman mode of ZnOEC (Figure 2) is seen to consist of two modes at 1538 and 1529 cm^{-1} (Figure 5).

Effects of Methine Deuteration. Figure 6 shows the IR spectra of CuOEC, CuOEC-γ,δ-d_2, CuOEC-α,β-d_2, and CuOEC-d_4 in CCl_4 solution. Figure 7 shows the resonance Raman spectra obtained with Q_y excitation at 615.0 nm of the same complexes

(32) Kincaid, J. R.; Urban, M. W.; Watanabe, T.; Nakamoto, K. *J. Phys. Chem.* **1983**, *87*, 3096-3101.

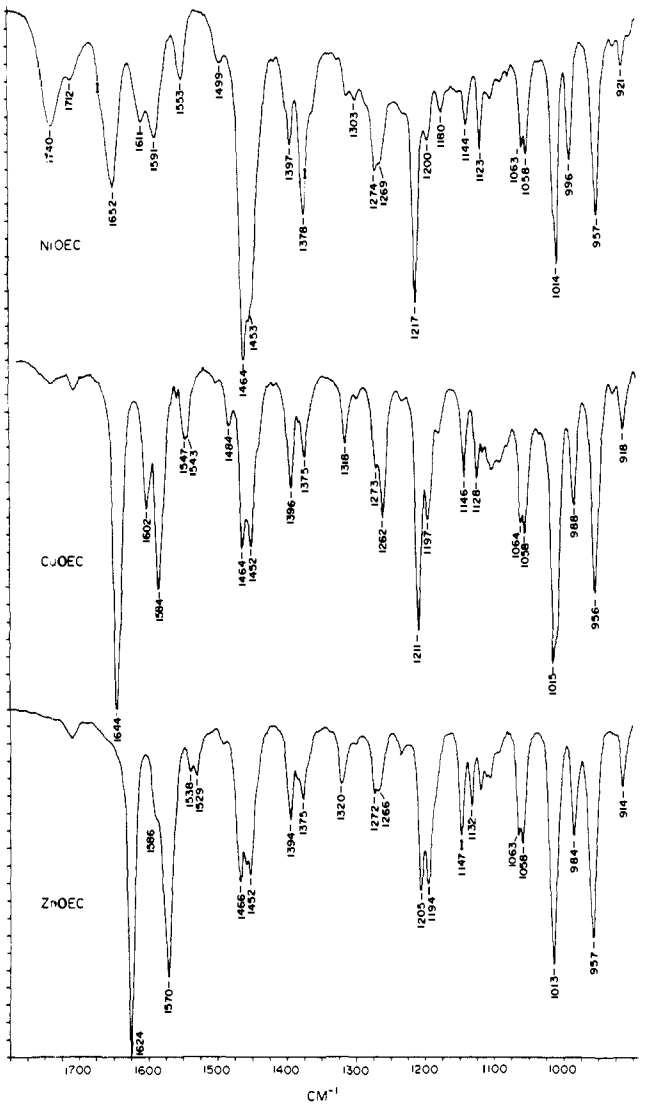

Figure 5. IR spectra of saturated CCl_4 solutions of ZnOEC, CuOEC, and NiOEC.

in CH_2Cl_2 solution. Different patterns of frequency shifts are observed for deuteration at the α,β positions relative to deuteration at the γ,δ positions. The effect of selective d_2 and d_4 methine deuteration for the high-frequency modes is summarized in Table III. The 1644-, 1602-, 1584-, 1507-, and 1486-cm^{-1} modes of CuOEC exhibit frequency shifts upon both α,β and γ,δ deuteration that are additive for CuOEC-d_4. Only the 1584- and 1507-cm^{-1} modes show equal frequency shifts upon α,β and γ,δ deuteration. The 1644- and 1486-cm^{-1} modes are more sensitive to γ,δ deuteration whereas the 1602-cm^{-1} mode shows a large shift upon α,β deuteration. The 1543-cm^{-1} mode shows no shift upon α,β deuteration but a shift of -17 cm^{-1} upon γ,δ and d_4 methine deuteration.

Below 1350 cm^{-1}, many of the vibrational modes of CuOEC are observed to be sensitive to methine deuteration. The complicated pattern of frequency shifts observed for CuOEC-α,β-d_2, CuOEC-γ,δ-d_2 and CuOEC-d_4 does not permit a 1:1 correlation of these modes in the various CuOEC complexes. Nevertheless, several modes clearly show α,β or γ,δ localization in this frequency region, as discussed in the following text.

The rationale for the experiments of Figures 6 and 7 was that selective d_2 methine deuteration would provide a direct test of the metallochlorin mode localization model advanced by Boldt et al.[21] This was based on the expectation that d_2 deuteration would shift a delocalized mode by half the amount that methine d_4 deuteration produced; a localized mode would exhibit distinctly different behavior that would be consistent with its specific mode composition. To test these predictions and to interpret the frequency

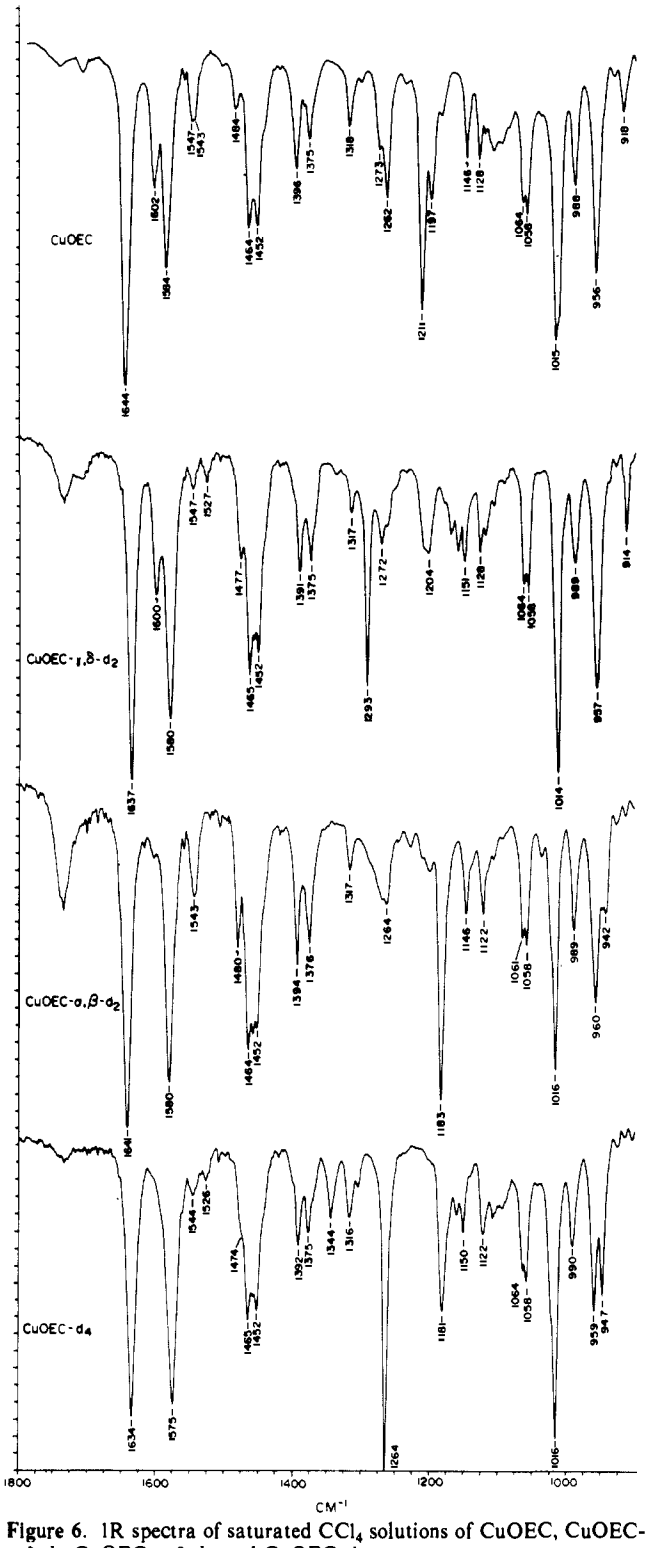

Figure 6. IR spectra of saturated CCl_4 solutions of CuOEC, CuOEC-γ,δ-d_2, CuOEC-α,β-d_2, and CuOEC-d_4.

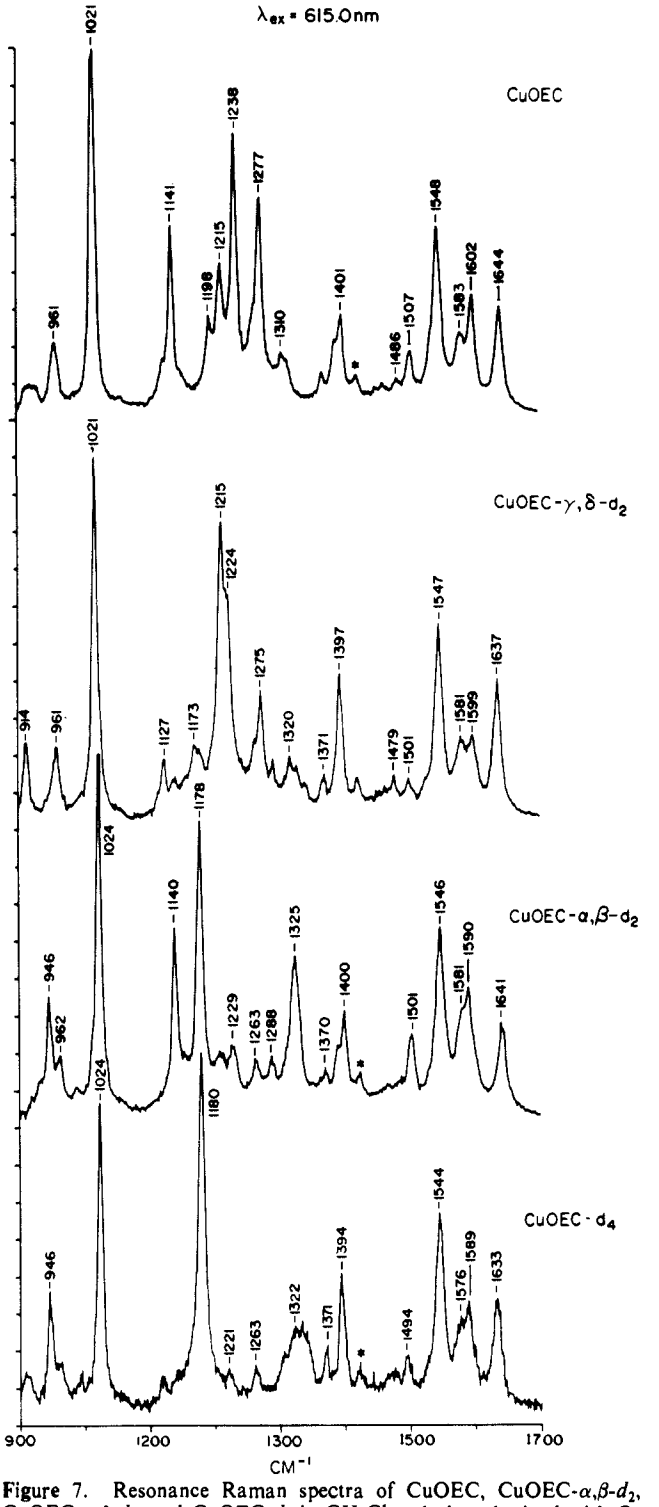

Figure 7. Resonance Raman spectra of CuOEC, CuOEC-α,β-d_2, CuOEC-γ,δ-d_2, and CuOEC-d_4 in CH_2Cl_2 solution obtained with Q_y excitation at 615.0 nm. Laser power: 40 mW. Concentration: ~60 μM.

shifts for the various methine-deuterated copper chlorin complexes, two methine-deuterated copper porphyrin compounds were prepared. In the CuOEP-d_4 species, all four methine carbons are deuterated; in the CuOEP-d_2 complex only two of the four bridging carbons are deuterium-substituted and these occur for adjacent methine positions. These compounds allows us to assess the effect of full and partial deuteration on modes that are delocalized throughout the macrocycle. Figure 8 shows the resonance Raman spectra of CuOEP, CuOEP-d_2, and CuOEP-d_4 with Soret excitation at 406.7 nm. Resonance Raman spectra of these complexes were also recorded with visible excitation at 514.5 nm (data not shown). Table IV indicates that the C_aC_m stretching modes ν_{10}, ν_{19}, and ν_3 of CuOEP show frequency shifts of −13, −22, and −10 cm^{-1} in CuOEP-d_4. For CuOEP-d_2, the frequency shifts of the ν_{10} and ν_3 modes are half of those observed for CuOEP-d_4. The ν_{19} mode shows a −14 cm^{-1} shift for CuOEP-d_2 but only a further −8 cm^{-1} shift for CuOEP-d_4. The frequencies of the C_bC_b stretching modes ν_2 and ν_{11} are not shifted upon d_2 or d_4 deuteration.[33] The results for the ν_3 and ν_{10} modes indicate that these vibrational modes are delocalized over the porphyrin macrocycle

(33) The ν_{11} mode appears as a shoulder on the broad ν_2 band in the resonance Raman spectra of CuOEP and CuOEP-d_2 with Soret excitation at 406.7 nm. With 363.8-nm excitation, the spectra of CuOEP and CuOEP-d_4 obtained by Oertling et al.[24] show an increase in the relative intensity of ν_{11} compared to ν_2 and no frequency shift upon d_4 methine deuteration.

Table II. Vibrational Frequencies (cm^{-1}) and Raman Depolarization Ratios of MOEC

NiOEC				CuOEC							ZnOEC	
RR				RR							RR	
406.7[a]	488.0	615.0	IR	406.7	ρ[b]	488.0	ρ	615.0	ρ	IR	406.7	IR
			1740							1741		
			1712							1708		1708
1651	1652	1652	1652	1644	0.8 dp	1643	0.5 p	1644	0.4 p	1644	1623	1624
1610	1613	1613	1611	1602	0.6 p	1601	1.0 ap	1602	0.5 p	1602	1587	1586
1588	1592	1589	1591	1584	0.4 p	1584	0.7 dp	1583	0.7 dp	1584	1570	1570
1554	1554	1554	1553	1547	0.3 p	1546	0.6 p	1548	0.4 p	1547	1534	1538
				1543	1.6 ap					1543		1529
1517	1517	1517		1507	0.2 p	1506	0.3 p	1507	0.4 p	1504	1491	1491
		1502	1499					1486	0.3 p	1484		
	1483											
1465	1466	1466	1464	1466	0.7 dp	1465	1.0 ap	1465	0.5 p	1464	1463	1466
			1457									1457
			1453							1452		1452
										1443	1440	1441
1403	1404	1401		1399	0.6 p	1402	0.7 dp	1401	0.5 p		1399	
			1397							1396		1394
1392				1388	0.3 p	1391		1392	0.4 p		1387	
	1383									1384		1383
			1378							1375		1375
1373	1373	1372		1372	0.3 p	1372	0.3 p	1373	0.3 p		1369	
1363	1363		1365	1361	0.3 p	1361	0.3 p				1359	
1349	1351			1352	0.2 p	1350	0.3 p				1349	
1316			1315	1318	0.6 p	1318	1.4 ap	1318	0.7 dp	1318	1320	1320
1307	1306	1308						1310	0.6 p			
			1303							1301		1301
1275	1275	1276	1274	1276	0.3 p	1275	0.7 dp	1277	0.4 p	1273	1275	1272
1266	1264	1266	1269	1266	0.3 p	1265	0.8 dp	1267		1262	1264	1266
1241		1239		1238	0.4 p			1238	0.4 p		1237	
			1233							1235		1235
1218	1219	1219	1217	1216	0.6 p	1212	0.6 p	1215	0.4 p	1211	1207	1205
1204	1202	1202	1200			1199	0.3 p	1198	0.3 p	1197	1198	1194
	1180		1180			1182	0.5 p			1183		1183
1154[c]	1154[c]			1155[c]		1157[c]		1154[c]			1158	
			1144							1146		1147
1142		1140		1141	0.3 p			1141	0.4 p		1141	
1125	1123	1124	1123	1129		1128	0.5 p	1128	0.5 p	1128		1132
										1119		1118
												1111
			1109							1107		1106
			1094							1095		1094
			1084							1086		
			1063							1064		1063
	1059		1058							1058		1058
1028	1027			1026	0.3 p	1026	0.3 p				1025	
1022	1022	1020		1021	0.5 p	1020	0.4 p	1021	0.4 p		1020	
			1014							1015		1013
		994	996							988		984
	960	961				960		961	0.4 p			
			957							956		957
932	932		932			932		932		932		
919	921	922	921					923		918		914
				909	0.3 p							

[a] 406.7, 488.0, and 615.0 refer to laser wavelengths (nm) used for Soret, Q_x, and Q_y excitation, respectively. [b] Key: ρ, depolarization ratio; p, polarized; dp, depolarized; ap, anomalously polarized. [c] Overlapped by CH_2Cl_2 solvent band.

and that their mode compositions are not altered by methine deuteration. The ν_{19} mode, although delocalized, is mixed with C_mH bending character[2d,e] and most likely changes in composition upon deuteration. Taken together, these results for partially and fully methine-deuterated CuOEP provide a basis for the analysis of the corresponding CuOEC complexes. Most importantly, they justify the expectation that, for a delocalized mode, methine d_2 deuteration can be expected to produce roughly half of the d_4 shift.

Resonance Raman Spectra of CuECI. For metalloporphyrins, the change in peripheral substituents that occurs upon going from CuOEP to CuEPI affects those modes with a contribution from C_bC_b and C_bC_s stretching and C_bC_s bending coordinates.[24] A similar dependence of the frequency of the analogous modes on peripheral substituents is expected for the metallochlorins and provides a means by which these modes may be identified. Figure 9 shows the resonance Raman spectra of CuECI in CH_2Cl_2 solution obtained with Soret excitation at 406.7 nm, Q_x excitation at 488.0 nm, and Q_y excitation at 615.0 nm. The 1584-, 1547-, and 1543-cm^{-1} modes of CuOEC show increases in frequency of 4, 4, and 3 cm^{-1}, respectively, as a result of the change in peripheral substituents in CuECI. In addition, the 1238-, 1215-, and 1198-cm^{-1} modes of CuOEC also exhibit increases in frequency. The change in peripheral substituents lowers the frequencies of the 1372-, 1361-, 1350-, and 1277-cm^{-1} modes of CuOEC by −4, −5, −3, and −7 cm^{-1}, respectively, whereas the 1021-cm^{-1} mode is replaced by two features at 998 and 982 cm^{-1} in CuECI.

Table III. Vibrational Frequencies (cm^{-1}),[a] Isotope Shifts (cm^{-1}),[a] and Structural Correlation Parameters for High-Frequency Metallochlorin C_aC_m and C_bC_b Normal Modes

		$\Delta\nu^b$					
NiOEC	CuOEC	α,β-d_2	γ,δ-d_2	d_4	$\Delta\nu_{subst}$[c]	K^d (cm^{-1}/Å)	A^d (Å)
1652	1644	−3	−7	−10	0	317	7.17
1613	1602	−12	−2	−13	0	282	7.67
1589	1584	−4	−4	−9	+4	237	8.67
1554	1547	−1	0	−3	+4	169	11.15
	1543	0	−17	−17	+3	270	7.71
1517	1507	−6	−6	−13	0	293	7.14
1502	1486	−4	−7	−10	0	381	6.90
1483							

	normal-coordinate analysis results for NiOEC[f]			
assignment[e]	no.	obsd	calcd	assignment
$\nu(C_aC_m)(\gamma,\delta)$, $\nu(C_aC_m)(\alpha,\beta)$	1	1648	1649	$\nu(C_aC_m)(\gamma,\delta)$
	2	1644	1637	$\nu(C_aC_m)(\gamma,\delta)$
$\nu(C_aC_m)(\alpha,\beta)$	3	1614	1618	$\nu(C_aC_m)(\alpha,\beta)$
	4	1608	1561	$\nu(C_bC_b)$(I,III)
$\nu(C_bC_b)$, $\nu(C_aC_m)(\alpha,\beta,\gamma,\delta)$	5	1590	1607	$\nu(C_aC_m)(\alpha,\beta)$
	6	1572	1557	$\nu(C_bC_b)$(I,III)
$\nu(C_bC_b)$	7	1546	1532	$\nu(C_bC_b)$(II), $\nu(C_aC_m)(\alpha,\beta)$
$\nu(C_aC_m)(\gamma,\delta)$, $\nu(C_bC_b)$	8		1540	$\nu(C_aC_b)$(II), $\nu(C_aC_b)$(I,III)
$\nu(C_aC_m)(\alpha,\beta,\gamma,\delta)$	9	1512	1489	$\nu(C_aC_m)(\alpha,\beta,\gamma,\delta)$, $\nu(C_aC_b)$(I,II,III)
$\nu(C_aC_m)(\gamma,\delta)$, $\nu(C_aC_m)(\alpha,\beta)$	10	1492	1498	$\nu(C_aC_b)$(I,II,III)
	11	1478	1506	$\nu(C_aC_m)\alpha,\beta,\gamma,\delta)$, $\nu(C_aN)$(I,II)

[a] From λ_{ex} = 615.0 nm Raman data and IR data. [b] Frequency shift (cm^{-1}) upon selective deuteration. [c] $\Delta\nu_{subst}$ is the frequency shift on change of peripheral substituents from CuOEC to CuECI. [d] K and A are from the relation $\nu = K(A - d)$. [e] This work. [f] From ref 21.

Table IV. Vibrational Frequencies (cm^{-1}), Isotope Shifts (cm^{-1}), and Structural Correlation Parameters for High-Frequency Metalloporphyrin C_aC_m and C_bC_b Normal Modes

		$\Delta\nu^b$					
mode[a]	CuOEP	d_2	d_4	$\Delta\nu_{subst}$[c]	K^d (cm^{-1}/Å)	A^d (Å)	PED[a]
ν_{10}	1639	−6	−13	+3	405	6.05	$\nu(C_aC_m)$49, $\nu(C_aC_b)$17
ν_2	1591	+1	0	+6	236	8.74	$\nu(C_bC_b)$60, $\nu(C_bEt)$19
ν_{19}[e]	1584	−14	−22		449	5.53	$\nu'(C_aC_m)$67, $\nu'(C_aC_b)$18
ν_{11}	1572	0	0[f]	+6	203	9.73	$\nu(C_bC_b)$57, $\nu(C_bEt)$16
ν_3	1505	−5	−10	+2	382	5.94	$\nu(C_aC_m)$41, $\nu(C_aC_b)$35
ν_{37}							$\nu(C_bC_b)$57, $\nu(C_bEt)$16[g]
ν_{38}	1554[h]				426	5.66	$\nu(C_aC_m)$34, $\nu'(C_aC_m)$24[g]
ν_{39}	1483[h]				278	7.34	$\nu'(C_aC_m)$36, $\nu'(C_aN)$17

[a] Mode designation and potential energy distribution (PED) from the normal-coordinate analysis of NiOEP.[2a] All of the metalloporphyrin normal-coordinate calculations cited in ref 2 agree as to the principal internal coordinate comprising these normal modes. In general, the differences in the detailed PED obtained by the three groups are not significant to our analysis of metallochlorin vibrations. [b] Frequency shift (cm^{-1}) upon selective deuteration. [c] $\Delta\nu_{subst}$ is the frequency shift on change of peripheral substituents from CuOEP to CuEPI.[24] [d] Calculated for ZnOEP, CuOEP, and NiOEP[37] by using $\nu = K(A - d)$. [e] Obtained from resonance Raman spectra with 514.5-mm excitation (data not shown). [f] See ref 33. [g] PED values for ν_{37} and ν_{38} have been interchanged.[32] [h] From ref 32.

Discussion

C_aC_m and C_bC_b Modes. In metallochlorins, the molecular symmetry is lowered to C_2 from D_{4h} for a planar metalloporphyrin macrocycle. Under C_2 symmetry, the resonance Raman active and IR active vibrational modes belong to the A and B symmetry species. The resonance Raman active polarized A_{1g} and depolarized B_{1g} modes of D_{4h} symmetry are expected to produce polarized modes of A symmetry in C_2. The anomalously polarized A_{2g} and depolarized B_{2g} modes correlate with depolarized B modes. The IR active E_u modes split into A and B symmetry species. The A and B modes are both IR and Raman active. If the porphyrin-mode composition is maintained in the chlorin complexes, eight C_aC_m stretching (4A + 4B) and four C_bC_b stretching (2A + 2B) modes are expected for a metallochlorin on the basis of the NiOEP normal-coordinate analysis.[2] Four of the C_aC_m and two of the C_bC_b stretching modes are derived from E_u modes.

In agreement with the mode-localization analysis of Boldt et al.,[21] our results indicate that such a symmetry-lowering approach does not adequately account for the vibrational-mode assignments for the metallochlorins. For these compounds we find that there is mixing of C_aC_m and C_bC_b stretching character in the high-frequency modes that is not prediced by direct comparison with the normal modes of NiOEP. For example, the 1584- and 1543-cm^{-1} modes of CuOEC are sensitive both to methine deuteration and to the difference in peripheral substituents for OEC and ECl. The frequency shifts observed for CuOEC-d_4 and CuECI (Table III) can be compared to those of the analogous porphyrin species, CuOEP-d_4 and CuEPI (Table IV). In CuOEP-d_4, the C_aC_m stretching modes ν_{10}, ν_{19}, and ν_3 exhibit frequency shifts of −13, −22, and −10 cm^{-1} with respect to those of CuOEP, but the C_bC_b stretching modes ν_2 and ν_{11} are unaffected. In addition, Kincaid et al.[32] observed −11- and −7-cm^{-1} shifts for the C_aC_m stretching modes ν_{38} and ν_{39} from the IR spectra of NiOEP and NiOEP-d_4. The 1644-, 1602-, 1584-, 1543-, 1507-, and 1486-cm^{-1} modes of CuOEC show substantial frequency shifts of −10, −13, −9, −17, −13, and −10 cm^{-1} upon d_4 methine deuteration. The magnitude of the frequency shifts indicates that these modes contain C_aC_m stretching character. Comparison of the resonance Raman spectra of CuOEP with CuEPI showed that a change in peripheral substituents resulted in an increase in frequency of the C_bC_b stretching modes ν_2 and ν_{11} by 6 cm^{-1}.[24] For CuOEC, we observe that the 1584-, 1547-, and 1543-cm^{-1} modes increase in frequency by 4, 4, and 3 cm^{-1} in CuECI. These modes are therefore predicted to contain C_bC3b stretching character. Thus, unlike the situation in metalloporphyrins, the methine-deuteration behavior and peripheral substituent dependence of the 1584- and 1543-cm^{-1} modes demonstrate that there is mixing of the $\nu(C_aC_m)$ and $\nu(C_bC_b)$ internal coordinates.

The mode characters we deduce from d_4 methine deuteration and the change in peripheral substituents are also reflected by the sensitivity to metal substitution. In the frequency region from

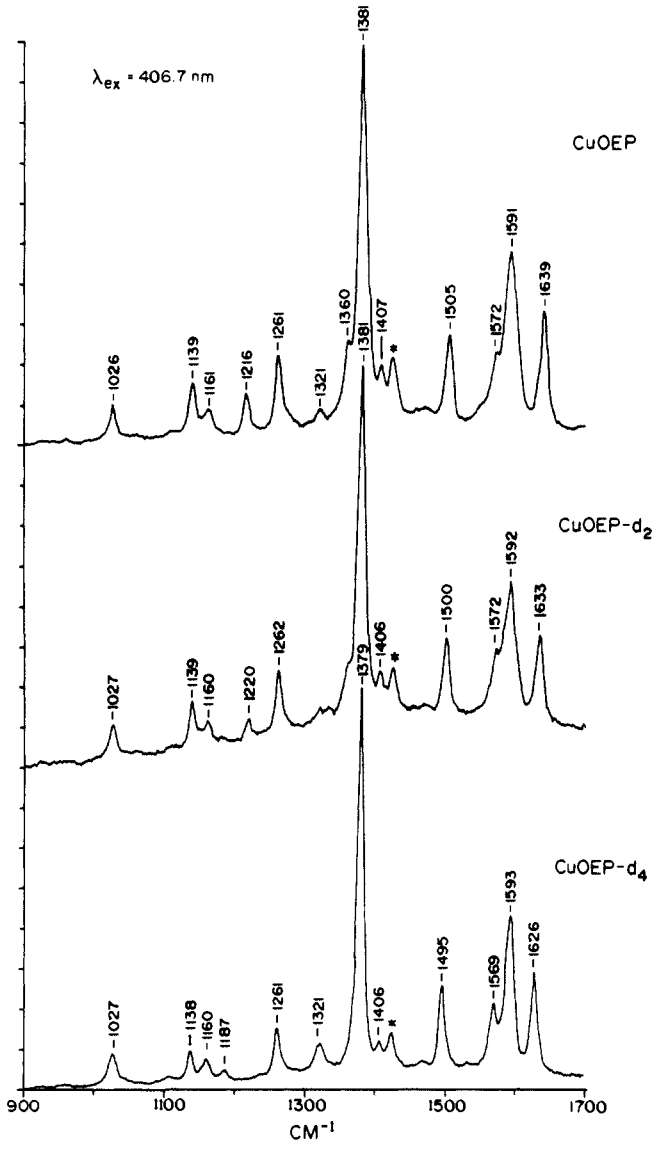

Figure 8. Resonance Raman spectra of CuOEP, CuOEP-d_2, and CuOEP-d_4 in CH_2Cl_2 solution obtained with Soret excitation at 406.7 nm. Laser power: 10 mW. Concentration: ~40 μM.

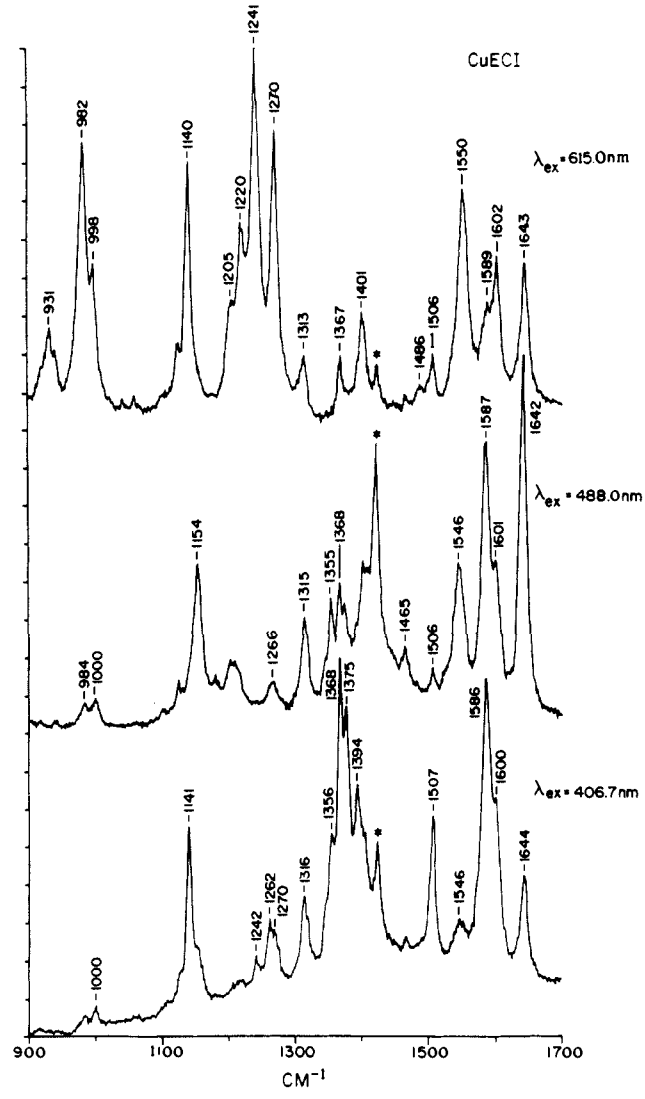

Figure 9. Resonance Raman spectra of CuECl in CH_2Cl_2 solution obtained with Soret, Q_x, and Q_y excitation. Laser powers: 6, 70, and 40 mW, respectively. Concentrations: 70, 800, and 40 μM, respectively.

1475 to 1700 cm^{-1}, seven modes corresponding to the 1644-, 1602-, 1584-, 1547-, 1543-, 1507-, and 1486-cm^{-1} modes of CuOEC are observed to be core size dependent. The relationship between vibrational frequency and core size of a metalloporphyrin often follows the empirical expression[34]

$$\nu = K(A - d)$$

where ν is the vibrational frequency (cm^{-1}), d is the center to nitrogen distance or core size of the metalloporphyrin (Å), and K (cm^{-1}/Å) and A (Å) are parameters characteristic of the macrocycle. The physically useful parameter is the inverse slope or K value, which is proportional to the amount of C_aC_m stretching character in the vibrational mode. Kitagawa and co-workers[14a] have previously applied this kind of analysis to metallochlorins; they achieved core size variation by working primarily with iron complexes in different spin and oxidation states. The iron chlorins, however, are susceptible to the same sorts of difficulties in such an analysis as are encountered with the corresponding iron porphyrins,[35] and for this reason, we have carried out our analysis for metals other than iron.[36] The core size correlation parameters, K and A, are listed in Tables III and IV for the high-frequency modes of the Ni, Cu, and Zn complexes of OEC and OEP, respectively. The same core sizes are assumed for the porphyrin and chlorin complexes, namely Ni (1.958 Å),[38] Cu (2.000 Å),[39] and Zn (2.047 Å).[40] From the metallochlorin K values, the 1644-, 1602-, 1543-, 1507-, and 1486-cm^{-1} modes of CuOEC have substantial C_aC_m stretching character, whereas for the 1584- and 1547-cm^{-1} modes contribution from the C_bC_b stretching coordinate is more apparent.

This vibrational frequency/core size analysis, however, is an oversimplification for two reasons. First, due to a sparcity of available crystal structures for metallochlorins (in particular a Cu^{2+} complex) we are forced to estimate d values from porphyrin structures. Second, the solution structure of NiOEC is known to be S_4 ruffled.[41] Such distortions will affect both the core size

(34) (a) Spaulding, L. D.; Chang, C. C.; Yu, N.-T.; Felton, R. H. *J. Am. Chem. Soc.* **1975**, *97*, 2517–2524. (b) Huong, P. V.; Pommier, J.-C. *C. R. Acad. Sci. Paris* **1977**, *C285*, 519–522.

(35) (a) Spiro, T. G.; Stong, J. D.; Stein, P. *J. Am. Chem. Soc.* **1979**, *101*, 2648–2655. (b) Choi, S.; Spiro, T. G.; Langry, K. C.; Smith, K. M.; Budd, D. L.; La Mar, G. N. *J. Am. Chem. Soc.* **1982**, *104*, 4345–4351.

(36) The frequencies predicted for CuOEC and ZnOEC based on the FeOEC core size correlation parameters of Ozaki et al.[13] are too low (CuOEC, 1633, 1593, 1579, 1538, and 1500 cm^{-1}; ZnOEC, 1611, 1574, 1564, 1521, and 1484 cm^{-1}).

(37) Kitagawa, T.; Ogoshi, H.; Watanabe, E.; Yoshida, Z. *J. Phys. Chem.* **1975**, *79*, 2629–2635.

(38) Cullen, D. L.; Meyer, E. F., Jr. *J. Am. Chem. Soc.* **1974**, *96*, 2095–2102.

(39) Moustakali, I.; Tulinsky, A. *J. Am. Chem. Soc.* **1973**, *95*, 6811–6815.

(40) Collins, D. M.; Hoard, J. L. *J. Am. Chem. Soc.* **1970**, *92*, 3761–3771.

(41) (a) Stolzenberg, A. M.; Stershic, M. T. *Inorg. Chem.* **1987**, *26*, 1970–1977. (b) Stolzenberg, A. M.; Stershic, M. T. *J. Am. Chem. Soc.* **1988**, *110*, 6391–6402.

Table V. Resonance Raman Frequencies (cm^{-1}) and Isotope Shifts (cm^{-1}) for Metallochlorin C_aN Normal Modes[a]

				normal-coordinate analysis results for NiOEC[d]			
NiOEC	CuOEC	$\Delta\nu$,[b] $^{15}N_4$	$\Delta\nu_{subst}$[c]	no.	obsd	calcd	assignment
1404	1402	−1	0	14	1402	1489	$\nu(C_aC_b)$(I,II,III), $\nu(C_aN)$(I,III,IV)
1373	1372	−6	−4				
1363	1361	−5	−5	17	1367	1339	$\nu(C_aN)$(I,II,III,IV), $\nu(C_bC_b)$(I,II,III)
1306	1318	−5	−3	20	1308	1301	$\delta(C_mH)$(a,b), $\nu(C_aC_b)$(I,III)
1154	1157	−9	−3	27	1152	1147	$\nu(C_bEt)$(I,II,III), $\nu(C_aN)$
1123	1128	−19	−3	29	1124	1083	$\nu(C_bEt)$(I,II,III), $\delta(C_mC_aN)$(IV)

[a] From λ_{ex} = 488.0 nm spectra. [b] From ref 12. [c] This work. $\Delta\nu_{subst}$ is the frequency shift on change of peripheral substituents from CuOEC to CuECl. [d] From ref 21.

values as well as vibrational frequencies; however, they are not likely to change appreciably the potential energy distributions of the normal modes.[21,42] Because of the enhanced conformational flexibility of the Ni complexes (this is true of not only the chlorin but also porphyrin complexes) we have used CuOEC for our deuteration studies. The CuOEC complex is thought to be relatively planar in solution.[41,43] A more refined vibrational structural analysis for the metallooctaethylchlorin system must await further X-ray crystal determinations and will be complicated by the inherent flexibility of the chlorin macrocycle. Indeed, we note substantial differences in vibrational frequencies of solution compared to solid-state (KBr pellets) samples, which suggest distinct structures.[44]

Despite these qualifications to the structural analysis, the above results show that the mode characters we observe for the high-frequency modes of CuOEC cannot be assigned by direct comparison with the normal modes of NiOEP. The resonance Raman spectrum of CuOEC-γ,δ-d_2 reported by Ozaki et al.[12] showed no shift of the 1602-cm^{-1} mode of CuOEC upon γ,δ deuteration and led these authors to conclude that the 1602-cm^{-1} mode corresponded to the porphyrin ν_2 C_bC_b stretching mode. We observe that the 1602-cm^{-1} mode shifts to 1589 cm^{-1} in CuOEC-d_4, which indicates substantial C_aC_m stretching character. To reconcile these deuteration effects, we compared the frequency shifts for CuOEC-γ,δ-d_2, CuOEC-α,β-d_2, and CuOEC-d_4. As seen in Figures 6 and 7 and Table III, the high-frequency modes exhibit different patterns of shifts upon α,β and γ,δ deuteration. The large (−13-cm^{-1}) frequency shift of the 1602-cm^{-1} mode results from deuteration at the α,β positions, but deuteration at the γ,δ positions has little effect on the frequency of this mode. On the other hand, the 1543-cm^{-1} mode of CuOEC is shifted by −17 cm^{-1} upon γ,δ deuteration and is unaffected by deuteration at the α,β positions. Both the 1644- and 1486-cm^{-1} modes of CuOEC show unequal frequency shifts upon α,β and γ,δ deuteration, with the larger shift resulting from γ,δ deuteration. The frequency shifts upon deuteration that we observe for CuOEC support the idea of mode localization in metallochlorins as proposed by Boldt et al.[21] from their study of NiOEC.

In Table III, we compare our results with the assignments of Boldt et al.[21] for NiOEC. CuOEC was chosen as our reference molecule, since it is presumed to be planar in solution, unlike NiOEC, which is ruffled.[41,43] Before proceeding to our analysis, we note that differences occur in the number and frequencies of the resonance Raman modes of NiOEC in Na_2SO_4 and in CH_2Cl_2 solution reported here. The 1644-, 1608-, and 1572-cm^{-} modes of NiOEC in Na_2SO_4 pellets are not observed in either the resonance Raman or the IR spectra of NiOEC in solution and appear to arise from altered conformations that are produced in the pelleting process.[44] These modes are not considered further in this analysis.

The 1648-, 1614-, and 1512-cm^{-1} modes of NiOEC in Na_2SO_4 were assigned by Boldt et al.[21] to C_aC_m stretching modes that are γ,δ localized, α,β localized, and delocalized, respectively. In CuOEC, we observe the analogous modes at 1644, 1602, and 1507 cm^{-1}. From their methine d_4 shifts and apparent insensitivity to changes in peripheral substituents at the C_b positions, these modes are assigned to C_aC_m stretching vibrations in agreement with Boldt et al.[21] Furthermore, the observation of equal and additive frequency shifts upon α,β and γ,δ deuteration shows that the 1507-cm^{-1} mode is delocalized over the chlorin macrocycle. Our deuteration shifts also confirm that the 1602-cm^{-1} mode is α,β localized. The 1644-cm^{-1} mode shows both α,β and γ,δ C_aC_m stretching character but with a greater localization in the γ,δ methines than in the α,β methines. This is a slight alteration from the assignment of Boldt et al.[21] who represented this mode as a 50:50 in-phase linear combination of the ν_{10} and ν_{37a} modes of NiOEP. Since we observe frequency shifts upon both α,β and γ,δ deuteration, a more accurate representation of this mode could be derived from a 50:20 in-phase combination of ν_{10} and ν_{37a}. The 1644- and 1507-cm^{-1} modes of CuOEC retain much of the character of the ν_{10} and ν_3 modes of NiOEP.

The compositions we deduce for the 1584- and 1486-cm^{-1} modes of CuOEC do not agree with those proposed by Boldt et al.[21] The 1584-cm^{-1} mode exhibits mixed C_bC_b and C_aC_m stretching character as judged by the intermediate K value, the +4-cm^{-1} shift upon change of peripheral substituents, and the −9-cm^{-1} shift upon d_4 deuteration. The equal −4-cm^{-1} shifts upon α,β and γ,δ deuteration indicate a delocalized mode. Bocian and co-workers[21] assigned the analogous 1590-cm^{-1} mode of NiOEC in Na_2SO_4 to C_aC_m stretching localized in the α,β methines. Disagreement is also found for the 1492-cm^{-1} mode of NiOEC in Na_2SO_4, which was assigned by Boldt et al.[21] to C_aC_b stretching localized in rings I–III. We observe the corresponding mode at 1486 cm^{-1} for CuOEC in CH_2Cl_2 solution with Q_y excitation. The high K value and −10-cm^{-1} shift upon d_4 deuteration indicate C_aC_m stretching rather than C_aC_b stretching character. The frequency shifts upon α,β and γ,δ deuteration show a greater γ,δ localization for this mode.

For CuOEC, we assign the 1547-cm^{-1} mode to C_bC_b stretching and the 1543-cm^{-1} mode to a mixture of C_bC_b stretching and γ,δ-localized C_aC_m stretching. The observation of these two modes in CuOEC is interesting since the normal-coordinate analysis[21] predicts four modes in this region at 1561, 1557, 1540, and 1532 cm^{-1}. Two of the modes (calculated at 1561 and 1557 cm^{-1}) are predicted to have C_bC_b stretching character, while the calculated 1540-cm^{-1} mode is predicted to have C_aC_b stretching character. In their resonance Raman spectra of NiOEC in Na_2SO_4 only a single mode at 1546 cm^{-1} was observed, and this mode did not shift in NiOEC-γ,δ-d_2. From these observations, the 1546-cm^{-1} mode of NiOEC was assigned by Boldt et al.[21] to C_bC_b and α,β-localized C_aC_m stretching calculated at 1532 cm^{-1}. The C_bC_b stretching character seen in the 1547- and 1543-cm^{-1} modes

(42) (a) Alden, R. G.; Crawford, B. A.; Ondrias, M. R.; Shelnutt, J. A. *Proceedings of the International Conference Raman Spectrosc. 11*, Clark, R. J. H., Long, D. A., Eds.; Wiley: New York, 1988; p 541. (b) Czernuszewicz, R. S.; Li, X.-Y.; Spiro, T. G. *J. Am. Chem. Soc.* **1989**, *111*, 7024–7031.

(43) Andersson, L. A.; Loehr, T. M.; Stershic, M. T.; Stolzenberg, A. M. *Inorg. Chem.* **1990**, *29*, 2278–2285.

(44) The high-frequency bands of NiOEC display an altered pattern of relative intensities for the solution and Na_2SO_4 pellet spectra with Soret excitation at 406.7 nm. In our spectra of NiOEC in KBr pellets, the 1572-cm^{-1} band increased in relative intensity as the ratio of NiOEC to KBr was lowered. This feature appears to arise from an anomalous component of the pellet sample. Resonance Raman spectra of CuOEC in KBr showed the same pattern of relative intensities as in solution with Soret, Q_x, and Q_y excitation. However, there are distinct shifts in frequency of the features in the 1450–1700-cm^{-1} region in solution versus KBr samples. That is, the CuOEC frequencies of 1644, 1602, 1584, and 1507 cm^{-1} in CH_2Cl_2 solution are shifted to 1632, 1598, 1582, 1539, and 1498 cm^{-1} in KBr. These imply a distinct conformational state in the pellet compared to the solution sample. Fonda, H. N.; Oertling, W. A.; Salehi, A.; Chang, C. K.; Babcock, G. T. In preparation.

Table VI. Resonance Raman Frequencies (cm^{-1}) and Isotope Shifts (cm^{-1}) for CuOEC Normal Modes in the Frequency Region below 1350 cm^{-1} [a]

CuOEC				metalloporphyrin mode[b]
h_4	α,β-d_2	γ,δ-d_2	d_4	
		α,β Localized		
1277		1275		
1215	946	1215	946	ν_{13}
	1325		1322	ν_{12}
	1178		1180	ν_{14}
		γ,δ Localized		
1238		1224		
1198				
		1173		
1141	1140	914	914	

[a] From λ_{ex} = 615.0 nm spectra. [b] NiOEP-mode numbers from ref 2, as described in the text. At least three α,β-localized modes in the metallochlorin system have analogies to the metalloporphyrin modes indicated.

supports the normal-coordinate analysis although the C_aC_m stretching character in the 1543-cm^{-1} mode has γ,δ localization and not α,β localization.

C_aN Modes. Under C_2 symmetry, six C_aN stretching modes would be expected for a metallochlorin.[45] The resonance Raman spectrum of CuOEC-$^{15}N_4$ recorded by Ozaki et al.[13] showed that the 1402-, 1372-, 1361-, 1318-, 1157-,[46] and 1128-cm^{-1} modes of CuOEC shifted by −1, −6, −5, −5, −9, and −19 cm^{-1}, respectively, upon $^{15}N_4$ substitution. These modes are therefore assigned to C_aN stretching. In Table V, we have summarized the Raman active modes observed for CuOEC and NiOEC in CH_2Cl_2 solution and for NiOEC in Na_2SO_4 along with the assignments proposed by Boldt et al.[21] from their normal-coordinate analysis. In this region, solution spectra gave somewhat better resolution than pellet data as the 1367-cm^{-1} mode of NiOEC in Na_2SO_4 (and in our spectra in KBr, not shown) has two components in CH_2Cl_2 solution at 1373 and 1363 cm^{-1}. Similarly, for CuOEC in KBr, we observe a single 1364-cm^{-1} mode that corresponds to the 1372- and 1361-cm^{-1} bands of CuOEC in solution.

The normal-coordinate analysis of NiOEC[21] indicates that there is mixing of the C_aN character with C_aC_b, C_bC_b, and C_bEt stretching coordinates. Table V collects CuOEC vibrational frequencies and shifts incurred by $^{15}N_4$ and substituent substitution. The involvement of the C_b atoms in these vibrational modes can be seen from the sensitivity of four of the modes to a change of peripheral substituents. The 1308- and 1124-cm^{-1} modes of NiOEC in Na_2SO_4 were assigned to modes 20 and 29, respectively, but the PED's have no contribution from C_aN stretching. In order to account for the observed $^{15}N_4$ frequency shifts, it would perhaps be better to assign the 1318-cm^{-1} mode of CuOEC to mode number 19 ($\nu(C_aN)$(I,III,IV), $\delta(C_mH)(\gamma,\delta)$) and the 1128-$cm^{-1}$ mode to number 28 ($\nu(C_bEt)$(I,II,III), $\nu(C_aN)$(I,III)).

C_mH Modes. Boldt et al.[21] used their normal-coordinate analysis of the C_mH bending region of the NiOEC spectrum to conclude the following: (a) the methine, γ,δ-hydrogen deformations are expected to be extensively mixed into a number of porphyrin skeletal modes, (b) the reduced ring C_bH bending motions couple with vibrations of the macrocycle and gain Raman intensity, and (c) the α,β-methine C_mH bending modes are likely to be relatively isolated and to exhibit behavior similar to, but simpler than, that of the methine C_mH bending modes in NiOEP. By comparing Q_x and Q_y spectra of NiOEC and NiOEC-γ,δ-d_2, they were able to test some of the above points, particularly a. The data presented here and in our earlier work on *trans*-CuOEC and CuMeOEC[47] allow us to extend and refine these conclusions.

The vibrational frequencies listed in Table VI illustrate that the α,β C_mH deformations show clear porphyrin-like behavior. Comparing the spectra of CuOEC and CuOEC-α,β-d_2 (Figure 7) reveals that the mode at 1215 cm^{-1} shifts to 946 cm^{-1} and an intense band at 1178 cm^{-1} appears upon deuteration. This behavior is analogous to that exhibited by the ν_{13} and ν_{14} modes of NiOEP.[2] Moreover, the appearance of the 1325-cm^{-1} mode in the CuOEC-α,β-d_2 spectrum reflects that of ν_{12} in NiOEP, which is usually not observed in the natural-abundance spectrum.[2a] Boldt et al.[21] predicted an α,β-localized mode at 1277 cm^{-1}, and the spectra in Figure 7 confirm this; this vibration, however, does not have a corresponding metalloporphyrin normal mode. The vibrational cordinates of the above four modes are α,β localized, as they are unperturbed by γ,δ-d_2 deuteration and their frequencies in the α,β-d_2 isotopomer persist virtually unchanged in the CuOEC-d_4 species. Some indication, however, that the α,β C_mH bending deformations contribute to more delocalized modes can be seen in the behavior of the cluster of modes in the 1190–1250-cm^{-1} region, which shows complicated intensity and frequency shifts in all three of the deuterated complexes relative to natural-abundance CuOEC.

Boldt et al.[21] have suggested that C_bH bending motions of ring IV contribute to Raman active modes at ~1230 and ~1200 cm^{-1} in NiOEC. Although deuteration of the reduced ring is the best way to test this idea, some insight can be gained into the extent of these C_bH contributions by comparing the spectra we have obtained for *trans*-CuOEC and CuMeOEC (Figure 3 parts a and b in ref 47). Fajer and co-workers have recently carried out an ESR/ENDOR/X-ray crystallographic analysis of the conformations of the zinc and cobalt complexes of *trans*-OEC and MeOEC and have found that substantial shifts in the C_aC_bH dihedral angle occur as the substituents on the reduced ring are varied.[48] Despite these differences in conformation, which are also expected for the copper complexes, our Raman spectra of *trans*-CuOEC and CuMeOEC in the 1000–1400-cm^{-1} region are similar. The only significant changes involve the mode at 1198 cm^{-1} in CuOEC (also seen in Figure 7), which appears to upshift and overlap the 1215-cm^{-1} mode resulting in a broad feature at ~1204 cm^{-1}, and 3–4-cm^{-1} shifts in modes at 1238 and 1155 cm^{-1} in the methyl-substituted derivative. While two of the above modes are in the regions indicated by Boldt et al.,[21] the extent of the shifts induced by perturbing the reduced ring by methyl substitution suggest that the degree of C_bH coupling into vibrations involving the π-conjugated macrocycle may not be as extensive as envisioned.

The γ,δ C_mH deformations were suggested to be extensively mixed with ring modes and thus to exhibit complex behavior.[21] Nonetheless, the data of Figure 7 provide several key insights into the characteristics of these motions. Upon γ,δ-d_2 deuteration, the mode at 1141 cm^{-1} disappears and new modes at 914 and 1173 cm^{-1} become apparent. The 1238-cm^{-1} mode apparently downshifts to 1224 cm^{-1} upon the same substitution. The behavior of the 1141- and 914-cm^{-1} modes indicates that these motions are strongly localized as their frequencies carry through essentially unchanged in the α,β-d_2 and d_4 species, respectively. A judgement as to the extent of localization of the 1173-cm^{-1} mode is rendered difficult since this region is obscured in Figure 7 by the strong α,β-localized 1180-cm^{-1} mode in the α,β-d_2 and d_4 species. Soret excitation data (not shown), however, suggest that this mode is also γ,δ-localized. As indicated above, the 1190–1250-cm^{-1} region is complex as modes that are extensively delocalized appear and respond in a complicated fashion under the various regimes of deuteration we have used. Nonetheless, it is clear that at least one (the 1238-cm^{-1} mode) and possibly another (the 1198-cm^{-1}

(45) The six C_aN stretching modes are derived from the ν_4, ν_{12}, ν_{20}, ν_{22}, and ν_{41} modes of NiOEP. The more recent normal-coordinate treatments of the E_u modes of NiOEP by Abe[2c] and Li et al.[2e] assign the PED of ν_{45} to C_aC_m stretching and not C_aN stretching as in ref 2a. The work of Spiro and co-workers[2e] further demonstrates a surprising amount of ethyl C–C stretching and C–H bending contributions to this and a large number of other normal modes.

(46) The 1157-cm^{-1} mode of CuOEC and 1154-cm^{-1} mode of NiOEC are overlapped by the 1154-cm^{-1} band of CH_2Cl_2. The presence of these modes is confirmed by resonance Raman spectra in KBr that show an 1155-cm^{-1} mode for CuOEC and an 1153-cm^{-1} mode for NiOEC.

(47) Salehi, A.; Oertling, W. A.; Fonda, H. N.; Babcock, G. T.; Chang, C. K. *Photochem. Photobiol.* **1988**, *48*, 525–530.

(48) (a) Forman, A.; Renner, M. W.; Fujita, E.; Barkigia, K. M.; Evans, M. C. W.; Smith, K. M.; Fajer, J. *Isr. J. Chem.* **1989**, *29*, 57–64. (b) Barkigia, K. M.; Fajer, J.; Chang, C. K.; Williams, G. J. B. *J. Am. Chem. Soc.* **1982**, *104*, 315–321.

mode) have γ,δ-C_mH contributions.

Table VI collects our information on the more prominent modes that have C_mH contributions. From the discussion above and the summary in the table, it is clear that normal modes with substantial contributions from C_mH deformations can be divided into three classes: (a) those that are localized to the α,β porphyrin-like part of the molecule, (b) those that are γ,δ localized, and (c) those that are substantially delocalized throughout the macrocycle. In this regard, the C_mH motions echo behavior that occurs for the skeletal motions themselves.

Ethyl Group Vibrations. The IR spectrum of CuOEC shows seven modes at 1464, 1452, 1375, 1064, 1058, 1015, and 956 cm^{-1} that are insensitive to metal substitution, methine deuteration, and a change in peripheral substituents and are therefore assigned to ethyl group vibrations. These modes are not observed in the resonance Raman spectra, except for the 1464-cm^{-1} mode that is present in nearly all of the resonance Raman spectra of the chlorin complexes that we have examined. The chlorin macrocycle does not appear to influence the internal vibrations of the ethyl groups greatly, since the frequencies are all close to the values reported by Kincaid et al.[32] from the IR spectrum of NiOEP in an argon matrix. However, a detailed vibrational analysis, using methylene-deuterated chlorin samples analogous to the OEP-d_{16} samples examined by Spiro and co-workers,[2e] will be necessary to establish this with certainty.

Conclusions

From our analysis of the resonance Raman and IR spectra of the MOEC complexes, we have shown that the vibrational modes of metallochlorins, while retaining many characteristics of metalloporphyrins including core size and peripheral substituent sensitivity, cannot be assigned by direct comparison with the normal modes of metalloporphyrins. The normal-coordinate analysis of NiOEC performed by Boldt et al.,[21] therefore, represents the starting point for the description of the vibrational modes of metallochlorins. In the work presented here, the mode compositions deduced for metallochlorins by metal substitution, methine deuteration, and a change in the peripheral substituents of OEC have been used to test their analysis. The overall agreement is surprisingly good, although some mode assignments need to be modified. Such agreement is gratifying, considering that it is the first normal-coordinate treatment of a metallochlorin and the data we have presented here may be used to refine it.

Abbreviations: DC = deuterochlorin IX dimethyl ester; diol chlorin = *cis*-3′,4′-dihydroxy-2,4-dimethyldeuterochlorin IX dimethyl ester; ECI = etiochlorin I; EPI = etioporphyrin I; Im = imidazole; IR = infrared; lactone chlorin = 5′-hydroxy-6,6′-*trans*-γ-spirolactone-2,4-dimethyldeuterochlorin IX monomethyl ester; $(Me)_7$chlorin = 3′-hydro-4′-methyl-2,4-dimethyldeuterochlorin IX dimethyl ester; OEC = octaethylchlorin, specifically, the trans derivative; OEP = octaethylporphyrin; pPP = photoprotoporphyrin IX dimethyl ester; RR = resonance Raman; TMC = *meso*-tetramethylchlorin; TPC = *meso*-tetraphenylchlorin; TPiBC = *meso*-tetraphenylisobacteriochlorin; TPP = *meso*-tetraphenylporphyrin.

Note Added in Proof. Kushmeider and Spiro (*J. Phys. Chem.*, in press) have recently completed a normal-coordinate analysis of NiOEC. They report the absence of mode localization and a clear correlation between chlorin and porphyrin modes. Their calculated meso-deuterium shifts, however, deviate noticeably from those we report here for CuOEC. Whether these deviations arise from mode-localization effects or from metal dependency in mode composition remains to be established.

Acknowledgment. We thank Professors D. Bocian and L. Andersson for helpful discussion and Prof. Andersson for communicating results in advance of publication. G.T.B. and C.K.C. acknowledge support from NIH Grants GM25480 and GM36520, respectively.

Concurrent Stepwise and Concerted Substitution Reactions of 4-Methoxybenzyl Derivatives and the Lifetime of the 4-Methoxybenzyl Carbocation

Tina L. Amyes and John P. Richard*

Contribution from the Department of Chemistry, University of Kentucky, Lexington, Kentucky 40506-0055. *Received March 2, 1990. Revised Manuscript Received August 14, 1990*

Abstract: The rates of reaction of 4-methoxybenzyl chloride, pentafluorobenzoate, and 3,5-dinitrobenzoate in 50:50 (v/v) trifluoroethanol/water are zero order in the concentration of azide ion. These reactions give good yields of the azide adduct from trapping of the 4-methoxybenzyl carbocation intermediate, and there is also strong common chloride ion inhibition of the reaction of 4-$MeOArCH_2Cl$. The yields of the azide and solvent adducts give the rate constant ratio $k_{az}/k_s = 25\ M^{-1}$, and analysis of the chloride common ion effect gives $k_{Cl}/k_s = 9\ M^{-1}$, for partitioning of the carbocation intermediate. The reaction of azide ion with the carbocation intermediate serves as a diffusion-controlled "clock" ($k_{az} = 5 \times 10^9\ M^{-1}\ s^{-1}$) for the reactions of solvent ($k_s = 2 \times 10^8\ s^{-1}$) and chloride ion ($k_{Cl} = 2 \times 10^9\ M^{-1}\ s^{-1}$). There is a solvent-induced change in mechanism and in the less ionizing solvents of 80:20 (v/v) and 70:30 (v/v) acetone/water; the reaction of azide ion with **1** produces the azide adduct by both trapping of the carbocation intermediate and by a concerted bimolecular substitution reaction.

Introduction

The substitution reactions of benzyl derivatives have been studied for most of this century, and these investigations have been central to the development of the theory of nucleophilic substitution at saturated carbon[1-3] and in the understanding of solvent effects on the mechanism of solvolysis reactions.[4] However, there are many unanswered questions regarding the precise mechanism for solvolysis in partially aqueous solvents, and the mechanism for the substitution reactions of 4-methoxybenzyl derivatives is particularly unclear.

(1) Streitwieser, A., Jr. *Solvolytic Displacement Reactions*; McGraw-Hill: New York, 1962. Thornton, E. R. *Solvolysis Mechanisms*; Ronald Press: New York, 1964.

(2) (a) Young, P. R.; Jencks, W. P. *J. Am. Chem. Soc.* **1979**, *101*, 3288-3294. (b) Harris, J. M.; Shafer, S. G.; Moffatt, J. R.; Becker, A. R. *Ibid.* **1979**, *101*, 3295-3300.

(3) Pross, A.; Shaik, S. S. *Acc. Chem. Res.* **1983**, *16*, 363-370.

(4) (a) Fainberg, A. H.; Winstein, S. *J. Am. Chem. Soc.* **1956**, *78*, 2770-2777. (b) da Roza, D. A.; Andrews, L. J.; Keefer, R. M. *Ibid.* **1973**, *95*, 7003-7009. (c) Schadt, F. L.; Bentley, T. W.; Schleyer, P. v. R. *Ibid.* **1976**, *98*, 7667-7674. (d) Kaspi, J.; Rappoport, Z. *Tetrahedron Lett.* **1977**, 2035-2038.

0002-7863/90/1512-9507$02.50/0